

Improved Techniques for Freeway Surveillance

HAROLD J. PAYNE, DAVID BROWN, AND STEPHEN L. COHEN

Surveillance of traffic conditions using presence detector data is essential for the operation of demand-responsive freeway control. Current operational practice aims to produce, by extremely simple means, estimates of volume and occupancy. An important step in the orderly development of metering strategies is the recognition that the processing of surveillance data should produce estimates of the traffic system states, namely, traffic densities and space-mean speeds in designated freeway sections. Several new techniques for freeway surveillance using modern estimation theory are presented. The approach adopted here is suboptimal using steady-state Kalman filters. The outstanding features of these estimators are their simple structure, light computational burden, and adequate performance to support effective demand-responsive control. The microscopic simulation program INTRAS was used to generate detector data to test the estimators.

Surveillance of traffic conditions using presence detector data is essential for the operation of demand-responsive freeway control. An important step in the orderly development of metering strategies is the recognition that the processing of surveillance data should produce estimates of traffic system states, specifically, traffic densities and space-mean speeds in designated freeway sections.

In contrast, current operational practice aims to produce, by extremely simple means, estimates of volume and occupancy. The principal defect of this approach is that occupancy depends on traffic operational and surveillance system hardware features. Furthermore, the approach fails to extract as much information as is available through more sophisticated processing.

Some new techniques for freeway surveillance using modern estimation theory are presented in this paper. Past state estimation efforts (1-5) have centered around developing optimal estimators. For example, Gazis and Szeto (5) developed an optimal estimator using traffic counts and speed measurements based on Kalman filter theory. The estimation approach adopted here is suboptimal using constant gain Kalman filters. Furthermore, Gazis and Szeto depended on the volume and occupancy measurements typically generated in operational surveillance systems. The performance improvements yielded are relative to current operational practice and entail a light computational burden and simple structure as compared to optimal state estimation methods. These estimators are able to accommodate the nonlinear state and measurement equations associated with freeway state estimation and produce adequate suboptimal performance to provide density and speed estimates

of sufficient quality to enable effective demand-responsive control.

The relationship of the state estimation surveillance function to the demand-responsive control problem is shown in Figure 1 where a control approach using a linear regulator from optimal control theory has been adopted (6). The regulator compares state estimates obtained from the surveillance software to expected traffic states to generate adjustments to the ramp metering rates.

The development and testing of improved algorithms to support the surveillance functions associated with demand-responsive ramp control are discussed in the remainder of this paper. First, the surveillance problem is defined in terms of the aggregate variables, dynamic equations, and measurement observables associated with a macroscopic freeway representation. The dynamical equations used by the estimators are the same equations used by the macroscopic simulation program FREFLO (7). Then, the algorithms for the improved state estimators are presented. A simple estimator is used for full-count detector stations with a more sophisticated estimator used in the case of partial-count detector stations. Lastly, the results of estimator testing on data sets generated by the microscopic simulation program INTRAS (8) are discussed.

SURVEILLANCE PROBLEM

The aggregate variables associated with the j th freeway section at time n are shown in Figure 2. The freeway segment is divided into sections defined by section boundaries at x_j , $j = 1, 2, \dots, N$. The time period is divided into uniform time intervals of length Δt . Within the j th section defined by the interval (x_{j-1}, x_j) , the following variables are defined.

- l_j = number of lanes,
- Δx_j = section length (miles),
- ρ_j^n = section density at time n (vehicles per lane per mile), and
- u_j^n = section space-mean speed at time n (miles per hour).

At the section boundaries, the following are defined:

- q_{j-1}^n = section entry flow rate over time slice n (vehicles per hour),
- q_j^n = section exit flow rate over time slice n (vehicles per hour), and
- θ_j^n = section exit occupancy over time slice n (percent).

H. J. Payne and D. Brown, VERAC Incorporated, 9605 Scranton Road, Suite 500, San Diego, Calif. 92121-1771. S. L. Cohen, Office of Safety and Traffic Operations Research and Development, Traffic Systems Division, FHWA, U.S. Department of Transportation, Room T201, Turner Fairbank Highway Research Center, 6300 Georgetown Pike, McLean, Va. 22101.

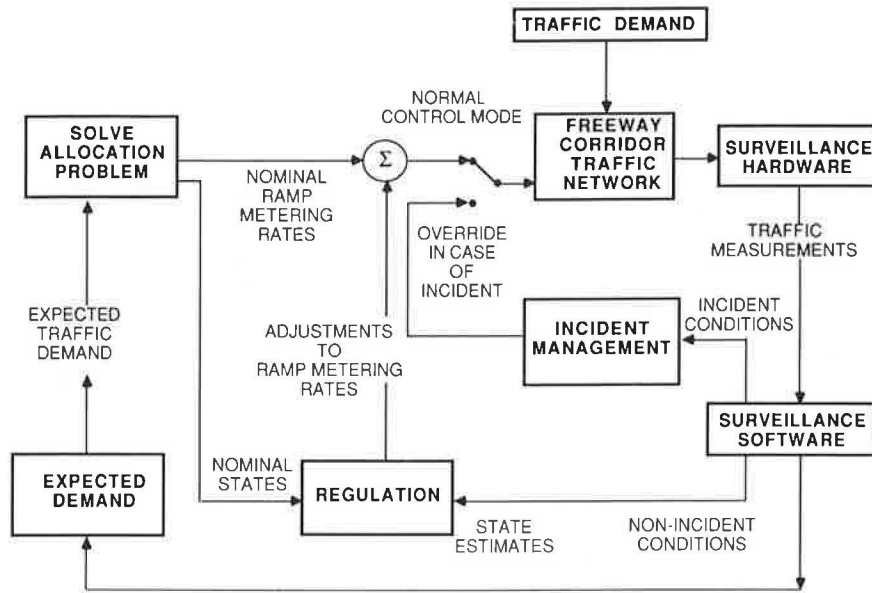


FIGURE 1 Relation of the surveillance state estimation function to demand-responsive control using a linear regulator approach.

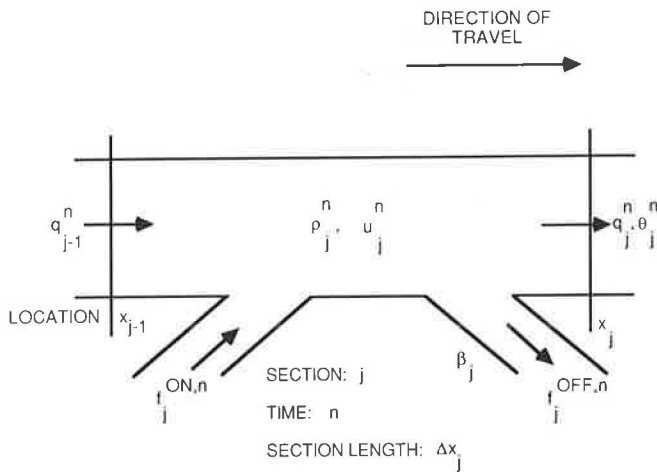


FIGURE 2 Aggregate variables.

Where appropriate, the following are defined:

- $f_j^{ON,n}$ = on-ramp flow rate over time slice n (vehicles per hour), and
- $f_j^{OFF,n}$ = off-ramp flow rate over time slice n (vehicles per hour).

This is the generic form of a section used by FREFLO (7). By definition, section boundaries coincide with detector station locations. Ideally, detector stations are located immediately upstream of on ramps and downstream of off ramps. In actual practice this may not be the case and more than one on or off ramp may exist in any given section. The FREFLO model may accommodate this situation by aggregating the effect of multiple on or off ramps. In addition, the FREFLO model will include an auxiliary lane in the section lane count l_j if the auxiliary lane is sufficiently long, relative to the section length, to have a pronounced effect on section dynamics.

Dynamic equations for density and speed are needed for the estimators. These are the discrete-time macromodel equations included in FREFLO. The first equation expresses the conservation of vehicles:

$$\rho_j^{n+1} = \rho_j^n + (\Delta t/l_j \Delta x_j) \times (q_{j-1}^{n+1} + f_j^{ON,n+1} - q_j^{n+1} - f_j^{OFF,n+1}) \quad (1)$$

The second equation is the dynamic speed relationship:

$$u_j^{n+1} = u_j^n + \Delta t \left[-u_j^n (u_j^n - u_e(\rho_j^n)/\Delta x_j) - (1/k_T \Delta x_j) \times (u_j^n - u_e(\rho_j^n)) - (K_v/K_T) (\rho_{j+1}^n - \rho_j^n)/\Delta x_j \right] \quad (2)$$

with boundary conditions $u_0^n = u_1^n$ and $\rho_{N+1}^n = \rho_N^n$

where

- K_T = relaxation coefficient (hours per mile),
- $u_e(\rho_j^n)$ = equilibrium speed for section j at density ρ_j^n , and
- k_v = anticipation coefficient (square miles per hour).

Use of the equilibrium relation to relate flow to density and speed is also helpful:

$$q_j^{n+1} = (1 - \beta_j) l_j \rho_j^{n+1} u_j^{n+1} \quad (3)$$

where β_j equals fraction of flow in section j , which exits the section via an off-ramp.

Freeway surveillance systems typically make measurements of flows and occupancies at loop detector stations located along the freeway. Loop detectors are deployed on freeways in three basic configurations: full-count stations, partial-count stations, and speed traps.

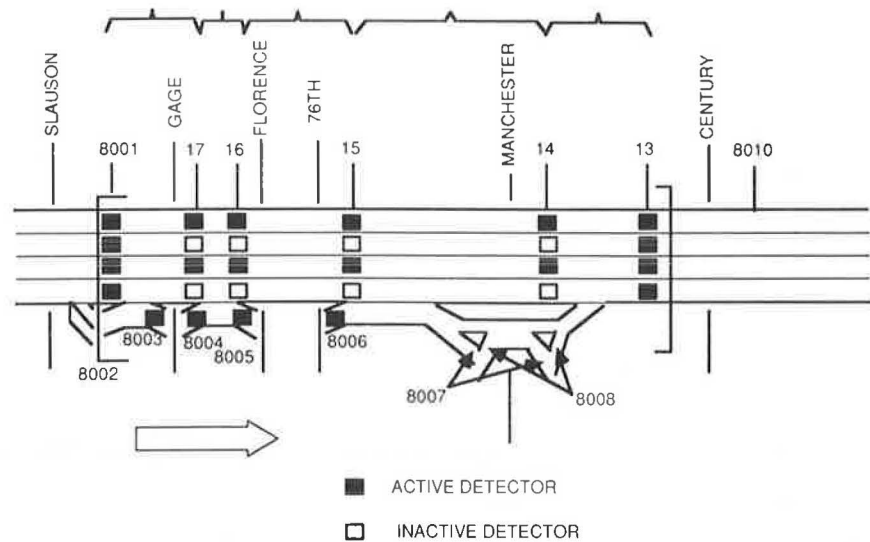


FIGURE 3 Surveillance sectionalization of a segment of the Harbor Freeway showing full- and partial-count sections.

A full-count station is a set of sensors placed at a given point on a freeway with one active detector in each lane. A partial-count station contains active detectors in some, but not all, lanes. Obviously, full-count stations provide a more accurate account of flow and occupancy at a given point in a freeway than partial-count stations. A speed trap contains two closely spaced detectors in a single lane. The purpose of the speed trap is to allow direct measurement of speed, which enables estimation of the reciprocal vehicle-sensor length (G -factor) that aids in density estimation.

The basic surveillance scheme is shown in Figure 3. The freeway segment is divided into sections with boundaries defined by detector count stations. For each individual section, a state estimator is used to estimate section density and space-mean speed from volume and occupancy measurements.

Given l_j noisy measurements of vehicle counts per lane, $z_{j,m}^{n+1}$, $m = 1, 2, \dots, l_j$, leaving section j over time slice $n+1$, the measurement equation for the volume leaving section j is formed as

$$\begin{aligned} z_j^{n+1} &= \sum_{m=1}^{l_j} a_{j,m} z_{j,m}^{n+1} = q_j^{n+1} + \alpha_j^{n+1} \\ &= (1 - \beta_j) l_j \rho_j^{n+1} u_j^{n+1} + \alpha_j^{n+1} \end{aligned} \quad (4)$$

where

$$\begin{aligned} a_{j,m} &= m\text{th lane exit flow rate measurement} \\ &\text{weighting factor } (a_{j,m} \geq 0), \text{ and} \\ \alpha_j^{n+1} &= \text{exit flow rate measurement error, section } j, \\ &\text{time slice } n+1. \end{aligned}$$

The purpose of the weighting factors is to compensate for partial count detector stations (the number of lanes with active presence sensors less than l_j). In this case, the weighting factors for the inactive lanes equal zero, and those for the active lanes are chosen to reflect the traffic distribution across the lanes at a given detector station. In the case of a full-count detector

station, the l_j weighting factors across the lanes are all chosen to equal 1.

Given l_j noisy measurements of lane occupancy, $\theta_{j,m}^{n+1}$, $m = 1, 2, \dots, l_j$, leaving section j over time slice $n+1$, the measurement equation for the occupancy in section j is formed as

$$\begin{aligned} \theta_j^{n+1} &= \left(\frac{\sum_{m=1}^{l_j} b_{j,m} \theta_{j,m}^{n+1}}{\sum_{m=1}^{l_j} b_{j,m}} \right) \\ &= (1/G)(1 - \beta_j)(l_j/l_{j+1}) \rho_j^{n+1} + \gamma_j^{n+1} \end{aligned} \quad (5)$$

where

$$\begin{aligned} b_{j,m} &= m\text{th lane exit occupancy measurement} \\ &\text{weighting factor, section } j \text{ } (0 \leq b_{j,m} \leq 1), \\ G &= \text{the mean reciprocal vehicle-sensor length} \\ &\text{relating occupancy to density, and} \\ \gamma_j^{n+1} &= \text{section occupancy measurement error for} \\ &\text{section } j, \text{ time slice } n+1. \end{aligned}$$

Note that the weighting factors $b_{j,m}$ are used for occupancy measurements to compensate for partial count detector stations. This measurement equation conforms to the off-ramp placement convention used by FREFLO and for surveillance testing on INTRAS data. In other words, if an off-ramp exists in a given freeway section it is located immediately upstream of the downstream section boundary.

ESTIMATORS

This section outlines the algorithms for the Single-Section Estimator (SSE), Multi-Section Estimator (MSE), and G -Factor Estimator (GFE). A complete development of these algorithms is described elsewhere (5).

SSE

The dynamic speed relation produces a model for a freeway segment consisting of coupled sections. In particular, the speed in a given section is modeled as a function of upstream speed and downstream density. Decoupling of the section parameters would allow a simple estimator to be used independently on each section. This is the approach used by the SSE. The conservation equation and standard equilibrium flow relation are used in lieu of the dynamic speed relation to yield a simple estimator depending only on first-order dynamics to estimate an individual section's density and speed independently of upstream or downstream parameters.

The SSE is actually composed of three estimators. Each estimator is executed separately in the following order: flow estimator, density estimator, speed estimator.

Assuming the volume measurement errors to be small in magnitude, zero mean, white, and mutually independent, a reasonable estimator for section volume is the weighted sum of the measured lane-vehicle counts.

$$\hat{q}_j^{n+1} = z_j^{n+1} \quad (6)$$

$$\hat{q}_{j-1}^{n+1} = z_{j-1}^{n+1} \quad (7)$$

The density estimator is determined from the steady-state solution to the scalar Kalman filter (9). Using the conservation equation to model the density dynamics, the density estimator then has the form

$$\hat{\rho}_j^{n+1} = \hat{\rho}_j^n + c_j^{n+1} + k(\theta_j^{n+1} - h\hat{\rho}_j^n - hc_j^{n+1}) \quad (8)$$

where

$$c_j^{n+1} = (\Delta t/l_j \Delta x_j)(\hat{q}_{j-1}^{n+1} + \hat{f}^{ON,n+1} - \hat{q}_j^{n+1} - \hat{f}_j^{OFF,n+1}),$$

$$\begin{aligned} k &= ph/(h^2p + r) = \text{steady-state gain,} \\ h &= (1 - \beta_j)(l_j/Gl_j - 1) = \text{measurement scalar,} \\ p &= (q + (q^2 + 4rq/h^2)^{1/2})/2 = \text{steady-state estimate error variance,} \\ r &= \text{var}(\gamma_j^{n+1}) = \text{measurement error, and} \\ q &= \text{variance of model error.} \end{aligned}$$

In Jazwinski's study (9), the first term of the right-hand side (RHS) is the previous density estimate; the second is the correction resulting from the net inflow into the section; the third provides a correction resulting from the discrepancy between the measurement and the previous density estimate.

Finally, the speed estimator in the SSE simply uses the estimates of density and volume in the equilibrium relationship to predict the new speed as

$$\hat{u}_j^{n+1} = \hat{q}_j^{n+1}/(1 - \beta_j)l_j \hat{\rho}_j^{n+1} \quad (9)$$

MSE

Nonuniformities in traffic flow and partial-count surveillance stations present potential sources of errors in estimating traffic parameters. In particular, nonuniformities in traffic flow here mean discontinuities in the gross features of the traffic stream, for example, as associated with the passage of a shock wave generated by a traffic incident. An MSE has the potential to overcome these problems.

A multi-section surveillance configuration for three contiguous sections of the freeway is shown in Figure 4. Note that the borders of the center section are depicted as having partial-count sensor stations. They could have equivalently been pictured as full-count sensor stations with a nonuniformity in traffic flow occurring in the center section. This example shows

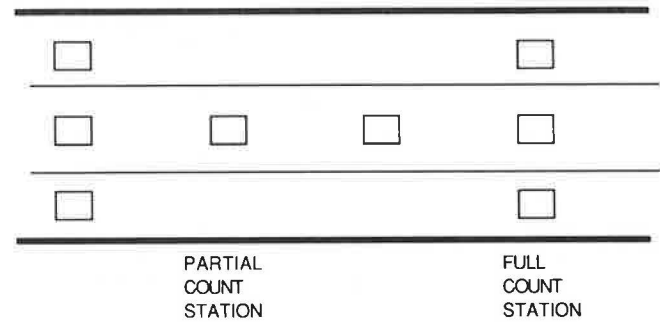


FIGURE 4 Multisection surveillance configuration.

principally that the volume and occupancy information either entering or leaving this section is poor. If the SSE is used on the center section, poor estimates of section density and speed will result because they are derived from volume and occupancy measurements having large errors. The concept of the MSE is to couple the three sections together through the dynamic equations so that good-quality information at the full-count sensor stations can be used to augment the information in the center section, which has only partial-count stations.

The MSE algorithm uses a constant gain Kalman filter to estimate section speeds and densities from noisy measurements of lane volumes and occupancies. The state consists of the densities and speeds for the N sections of the freeway segment of interest:

$$x^n = (\rho_1^n, u_1^n, \rho_2^n, u_2^n, \dots, \rho_N^n, u_N^n)^T \quad (10)$$

and the control consists of the m on-ramp flow rates in the freeway segment:

$$v^n = (f_1^{ON,n}, f_2^{ON,n}, \dots, f_m^{ON,n})^T \quad (11)$$

where $m \leq N$.

The state dynamics as defined by Equations 1 and 2 are nonlinear and may be linearized about a nominal state \underline{x}^* and control \underline{v}^* . The resultant first-order perturbation equations in vector form become (6)

$$\delta \underline{x}^{n+1} = A \delta \underline{x}^n + B \delta \underline{v}^n + \underline{w}^n \quad (12)$$

where

$$\begin{aligned}\delta \underline{x}^n &= \underline{x}^n - \underline{x}^*, \\ \delta \underline{v}^n &= \underline{v}^n - \underline{v}^*, \\ A &= \text{matrix of state partial derivatives,} \\ B &= \text{matrix of control partial derivatives, and} \\ \underline{w}^n &= \text{mismodeling noise process.}\end{aligned}$$

Similarly, the measurement equations as defined by Equations 4 and 5 are nonlinear and may also be linearized about nominal conditions:

$$\delta \underline{y}^{n+1} = H \delta \underline{x}^{n+1} + \underline{s}^{n+1} \quad (13)$$

where

$$\begin{aligned}\delta \underline{y}^{n+1} &= (\delta \theta_1^{n+1}, \dots, \delta \theta_N^{n+1}, \delta z_1^{n+1}, \dots, \delta z_N^{n+1})^T, \\ H &= \text{matrix of measurement partial derivatives,} \\ &\text{and} \\ \underline{s}^{n+1} &= \text{measurement of noise process.}\end{aligned}$$

Note $\{\underline{w}^n\}$ and $\{\underline{s}^n\}$ are assumed to be a mutually independent sequence of zero-mean, white, Gaussian noise with corresponding covariance Q and R .

Then, given the estimate at time n of the perturbation in the state $\delta \underline{x}^n = \underline{x}^n - \underline{x}^*$, the MSE estimates perturbations in the state at time $n+1$ to be

$$\delta \underline{x}^{n+1} = A \delta \underline{x}^n + B \delta \underline{v}^n + K(\delta \underline{y}^{n+1} - H A \delta \underline{x}^n - H B \delta \underline{v}^n) \quad (14)$$

where

$$\begin{aligned}K &= P H^T (H P H^T + R)^{-1}, \text{ the steady-state gain; and} \\ P &= A P A^T - A P H^T (H P H^T + R)^{-1} H P A^T + Q, \text{ the} \\ &\text{steady-state estimate error covariance.}\end{aligned}$$

The state estimate at time $n+1$ may be recovered by adding the nominal state to the perturbation estimate:

$$\underline{x}^{n+1} = \delta \underline{x}^{n+1} + \underline{x}^* \quad (15)$$

The nominal state (of section densities and speeds) is defined as the steady-state freeway condition associated with a given demand level. It is produced by running FREFLO to steady state using the on-ramp rates produced by the allocator for a given demand level and the origin-destination distribution (6). The nominal state is assumed constant over a 30-min time horizon because demand levels typically will not change appreciably over these time periods.

Note that the MSE (Equations 14 and 15) implies a very light, real-time computational burden because the steady-state gain is computed off line.

GFE

One of the principal sources of error involved in estimating traffic parameters is an inaccurate determination of the mean of the vehicle-sensor length distribution or its reciprocal, the G-factor (4). The accuracy with which the G-factor is determined directly affects the accuracy of all traffic parameter

estimates involving density or speed. It is therefore essential that a means be devised to provide an accurate determination of the G-factor. Moreover, it should be recognized that the G-factor will vary by location, even by lane, and with time will reflect both variations between detectors and variations in the composition of traffic, particularly in terms of the fraction of heavy-duty vehicles.

It is not possible to determine the G-factor in any direct way from data from a single presence detector. However, by using data from a pair of presence detectors (from a speed trap) it is possible to make measurements of individual vehicle-sensor lengths from which an estimate of the G-factor may be computed.

The G-factor is a scaled version of the reciprocal mean length of the vehicle-sensor length distribution. Because it is recognized that the mean vehicle-sensor length $\bar{\lambda}$ should be allowed to vary with time, it may be computed as a moving average over N samples. Given measurements (estimates) of the vehicle-sensor lengths, $\hat{\lambda}(i)$, $i = 1, 2, \dots$, associated with a particular speed trap, the moving average is specified by

$$\bar{\lambda}(n; N) = (1/N) \sum_{i=n-N+1}^n \hat{\lambda}(i), \quad n \geq N \quad (16)$$

This formulation suggests that distinct G-factors can be determined for distinct speed traps corresponding to different lanes on the freeway.

The estimate of the G-factor after the n th sample at the particular speed trap is then

$$\hat{G}(n; N) = 52.8 / \bar{\lambda}(n; N) \quad (17)$$

One disadvantage of using a moving average to estimate $\bar{\lambda}$, as in Equation (16), is the necessity of storing N measurements. This problem may be overcome by using a recursive form for the estimator (6).

TEST RESULTS

The results of surveillance algorithm testing using detector data produced by the microscopic traffic simulation program INTRAS (8) are described next. In lieu of real data, the benefits associated with estimator testing using INTRAS data are twofold:

1. INTRAS provides realistic representations of detector data compared to actual data produced by current freeway surveillance systems, and
2. INTRAS provides the true values of section space-mean speeds and densities associated with the detector data so estimator performance may be directly compared to truth.

The performance of three estimators for estimating freeway densities and speeds from volume and occupancy measurements can be compared using the INTRAS data sets. These three estimators are Scaled Occupancy Estimator (SOE), SSE, and MSE.

The SOE, which reflects the state estimator performance of current operational surveillance systems, uses scaled occupancy to compute density estimates:

$$\hat{\rho}_j^n = G\hat{\theta}_j^n \quad (18)$$

and the equilibrium relation to compute speed estimates:

$$\hat{u}_j^n = \hat{q}_j^n / (1 - \beta_j) I_j \hat{\rho}_j^n \quad (19)$$

The results of G-Factor Estimator (GFE) testing are presented next. The section begins with a description of the test scenarios and measurement generation methodology used for surveillance algorithm testing.

Test Scenarios

Surveillance testing was performed on a 30-min data set consisting of nonincident traffic flow data for the Shirley Highway generated by the microscopic simulation program INTRAS. A 5-mi section of the northbound Shirley Highway (I-395) in Arlington and Fairfax counties, Virginia, was chosen. Detector data were available from Nodes 8 to 22 on the highway (Figure 5). The location of the detector stations used for testing are indicated. Unless otherwise indicated, all detector stations are of the full-count, single-loop variety. Several full-count, double-loop detector stations (speedtraps) are included in the data set at Nodes 8 and 15.

The location of the detector stations is approximately coincident (6 ft downstream) with the network node locations. The detector locations define the boundaries of the sectionalization of the freeway, which correspond in this case to the link boundaries. The SOE, SSE, and MSE produce estimates of speed and density for each freeway section. The correspondence of section and link boundaries was chosen to facilitate comparison of section state estimates with known link aggregate speeds and densities.

The seven test scenarios used for surveillance algorithm testing on the INTRAS data sets are given in Table 1. Six scenarios were used for comparative testing of the SOE, SSE, and MSE, and one scenario was used for the GFE testing.

Generation of Measurements

The detector data generated from INTRAS come in the form of on and off times associated with a car passing through a

TABLE 1 TEST SCENARIOS FOR SURVEILLANCE ALGORITHM TESTING USING INTRAS DATA SETS

Estimator Type	Full-Count Detectors	Partial-Count Detectors
SOE	X	X
SSE	X	X
MSE	X	X
GFE	X	

presence detector. From these on/off times, the measurement software provides measurements of detector volumes (counts) and occupancies, which are used by the SOE, SSE, and MSE to estimate section density and speed. For the purpose of estimator testing, volumes and occupancies were produced every 30 sec from the INTRAS data. Consequently, the estimators will produce traffic state estimates every 30 sec coincident with the measurement times. The 30-sec sampling interval was chosen to facilitate comparison of state estimates with true states because the INTRAS truth values are also produced every 30 sec. Furthermore, the 30-sec sampling rate is a typical sampling

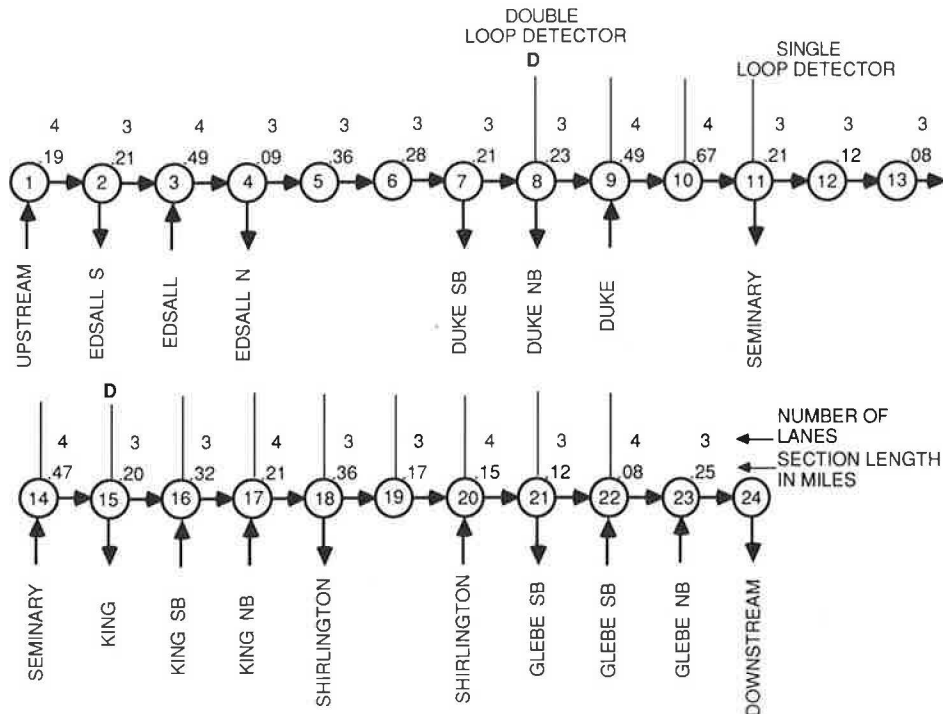


FIGURE 5 Network representation of I-395 (Shirley Highway), inbound in Virginia.

time for freeway surveillance systems. Additionally, similar estimation performance as illustrated here should be achievable for 1- to 2-min sampling rates.

Measurement volumes are determined from the number of counts that are registered at a detector over the 30-sec sampling interval. The flow measurements become the 30-sec counts multiplied by 120 (to yield flows in units of vehicles per lane hour) and are tagged with the time at the end of the sampling interval. Occupancy represents the percentage of time the detector is on (registering the presence of a car) during the 30-sec sampling interval.

Sample volume and occupancy measurements obtained from a detector station in the Shirley Highway data set generated by INTRAS are shown in Figure 6. The measurements are characterized by large variations in both volume and occupancy over time. These are typical measurement sets that are used by the

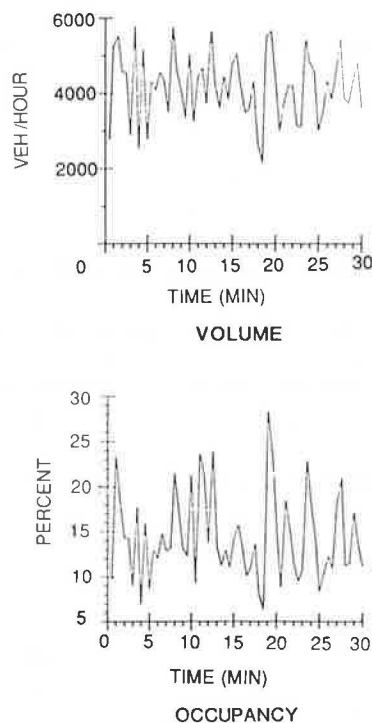


FIGURE 6 Sample volume and occupancy measurements from a detector station.

surveillance algorithms to estimate section space-mean speed and density.

Sections 3, 4, 5, and 6 were chosen as being representative of typical length sections encountered in real surveillance systems and correspond, respectively, to links (10,11), (11,14), (15,15), and (15,16) in Figure 5. The length of the sections vary from long (0.67 mi) to average (0.41 and 0.47 mi) to short (0.20 mi) for Sections 3, 4, 5, and 6, respectively. A constant G-factor ($G = 2.26$) was used for all plots and was determined empirically from the data set. A description of the determination of the G-factor and the resulting errors in density estimates that the errors in the parameter G induce follows.

The SSE clearly provides better density estimates (that is, closer agreement to truth) than the SOE for the long- and

medium-length sections (Sections 3, 4, 5). This is to be expected, because scaling the occupancy at the downstream section boundary cannot accurately reflect the section density when the section length exceeds the distance the cars can travel during the 30-sec count time. That is, some of the cars in the section at the beginning of the count time will not be able to traverse the length of the section and be registered at the downstream detector during the count time. The SSE uses an aggregate model based on the conservation of flow in and out of the section during the count time and is able to overcome this deficiency. The performance of the SSE and the SOE for density estimation on short sections (e.g., Section 6) are noted as similar.

Both the SSE and the SOE use the equilibrium equation to compute speed estimates from density and volume estimates. Additionally, both methods simply use measured counts for volume estimates. Thus, because the SSE is able to produce equal or better density estimates than the SOE, SSE speed estimates should be equal or better than those produced by the SOE. This claim is confirmed in Table 2, which gives the root mean square (rms) errors in density and speed estimates produced by the SSE and SOE for both full- and partial-count detector stations. These values represent the average error in

TABLE 2 RMS ERROR IN DENSITY AND SPEED ESTIMATES FOR SURVEILLANCE ALGORITHMS (Absolute/Percent)

Estimation Technique	Full-Count Detectors	Partial-Count Detectors
SOE	$\sigma_p = 8$ vplm/27% $\sigma_u = 12.8$ mph/28%	$\sigma_p = 9.4$ vplm/31% $\sigma_u = 17$ mph/38%
SSE	$\sigma_p = 6$ vplm/20% $\sigma_u = 7$ mph/15%	$\sigma_p = 7$ vplm/23% $\sigma_u = 10$ mph/22%
MSE	$\sigma_p = 5$ vplm/17% $\sigma_u = 3$ mph/7%	$\sigma_p = 5$ vplm/17% $\sigma_u = 3$ mph/7%

density and speed estimates observed over all 12 sections of the Shirley Highway data set. The average fluctuations in flow are 1,200 vph for full-count detector stations and 1,900 vph for partial-count stations.

As indicated in the table, the SSE produces better speed and density estimates than the SOE for both full- and partial-count detector stations. The SSE partial-count results, particularly the 10 mph speed error, are improved by the MSE.

The SSE and the MSE were compared in the partial-count detector station configuration where full-count stations are located every 1 to 2 mi with partial-count stations in between. Such conditions yield about the worst expected detector configuration to be found in practice. A partial-count station consists of a single active detector in the center lane. Results from Sections 3, 4, 5, and 6 of the Shirley Highway are used again for illustrative purposes. The estimation error is defined as the difference between the state estimate and the true value of the state as determined by INTRAS. Perfect state estimation would result in a zero estimation error for all time.

The improvements in both density and speed estimation of the MSE over the SSE for partial-count stations is evident from Table 2, which summarizes the root mean square errors in density and speed estimates produced for both full- and partial-count detector stations. These figures represent the average

error in density and speed estimates observed over all 12 sections of the Shirley Highway data set.

For the partial-count detector case, a dramatic reduction in speed error from 10 mph for the SSE to 3 mph for the MSE is noted. Substantial reductions in density error [7 vehicles per lane-mile (vplm) to 5 vplm] are also realized in switching from the SSE to the MSE. Additionally, as indicated by the results in Table 2, the MSE in the partial-count configuration outperforms the SSE in the full-count configuration. This is attributed to the use by the MSE of the dynamic speed equation in state estimation.

It was found that the full-count MSE estimation errors are practically identical to the partial-count MSE errors for both density and speed. This is a result of a measurement error induced by modeling volume at a detector station in terms of section density and space-mean speed through the equilibrium relation. This mismodeling error, due to the nonhomogeneity of real flow, dominates the measurement error induced by partial-count measurements. The equivalent MSE performance for full- and partial-count stations (Table 2) indicates that, due to model limitations, it is unnecessary to upgrade from partial- to full-count detector stations to realize the full potential of the MSE.

GFE Results

The G-factor was modeled as a constant both temporally and spatially along the freeway for this surveillance algorithm testing. The distribution of vehicles of various lengths in the INTRAS data sets was held constant over the simulation time period (see Table 3). Thus, all deviations in the G-factor were presumed to be white noise. If the time period had been divided into subintervals with varying inputs, holding the G-factor constant may not have resulted in such a good approximation. An assessment of the corresponding density estimation errors made by the surveillance algorithms using a constant as opposed to a temporally or spatially variable G-factor was then made.

The variation of the G-factor over all detectors displayed in the moving average plots is shown as follows with standard deviation of parameters indicated in parentheses.

<i>Data Set</i>	<i>Average G-Factor</i>	<i>Average rms Error</i>
Shirley Highway	2.26 (.005)	0.25 (0.31)

The average G-factor and average rms error in G-factor over all tested detectors for the respective data sets are listed. The standard deviations of these averages are also noted and are good indications of the spatial variation of these parameters. The small size of the standard deviations indicates little variation in the average G-factor or rms error in the G-factor (that is, temporal variation) from detector to detector. The errors induced in density estimation due to these small spatial variations are negligible and support the use of a spatially constant G-factor.

The temporal variation in the G-factor as indicated by the average rms error in the preceding table represents a substan-

tially larger error in density estimation results. For the Shirley Highway data set, the 0.25 rms error from using a constant G-factor translates into a 3-vplm density error for a 12 percent occupancy level, which is a typical occupancy for the Shirley Highway data set. However, the error in density estimation due to modeling the G-factor as temporally constant does not dominate the total density error, which at best is 5 vplm for the MSE. Other error sources (e.g., the volume measurement model) contribute the dominant portion of the error (4 vplm).

Thus, modeling of the G-factor as a constant induces relatively small errors in density estimates while contributing minimum estimator complexity to the surveillance algorithms. The specific G-factors and corresponding density errors presented here are only indicative of the INTRAS data sets. Different variations may occur under real freeway conditions due to less uniform vehicle length distributions.

TABLE 3 DISTRIBUTION OF VEHICLES OF VARIOUS LENGTHS IN INTRAS DATA SETS, SHIRLEY HIGHWAY

Vehicle Type	Vehicle Length (ft)	Distribution (%)
Low-performance passenger car	20	48
High-performance passenger car	20	48
Intercity bus	43	1
Heavy single-unit truck	26	2
Trailer truck	53	1

The G-factor estimator also has the ability to count vehicles of various lengths, such as trucks and buses, over time. This capability is shown in Figure 7. A single sample moving average was used to estimate the reciprocal vehicle-sensor length for each vehicle passing through the speed trap. The GFE easily discriminates among passenger cars, heavy single-unit trucks, intercity buses, and trailer trucks due to their different vehicle lengths. The GFE cannot discriminate between low-performance and high-performance passenger cars because they both have the same vehicle length.

CONCLUSIONS

The various surveillance algorithms observed over all 12 sections of the INTRAS data set indicate that

- The SSE produces better speed and density estimates than the SOE,
- The MSE is needed in partial-count detector situations especially for speed estimation,
- The performance of the MSE is substantially the same for partial and full-count detector stations, and
- The modeling of the G-factor as a constant induces relatively small errors in density estimates while contributing minimum estimator complexity to the surveillance algorithms.

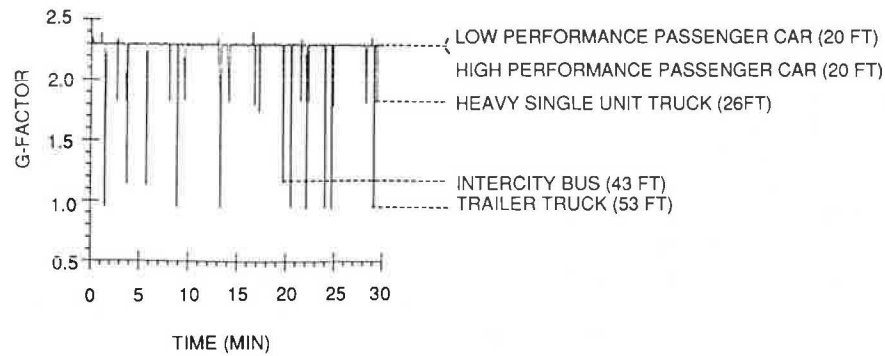


FIGURE 7 Ability of G-factor estimator to count trucks and buses.

In a recently completed study (6), development of a demand-responsive control strategy using a linear regulator from optimal control theory revealed that

- In light congestion, the regulator performance was insensitive to the level of surveillance hardware (density of detectors) and algorithm (SOE, SSE, and MSE), and
- In moderate congestion associated with constrained traffic conditions, a significant increase in regulator performance was achievable using superior-quality surveillance provided by the MSE.

Real traffic data needs to be examined to check these conclusions.

ACKNOWLEDGMENT

This research was sponsored by FHWA. The authors would like to thank Joan Todd and Louise Schwartz for their programming and analysis support.

REFERENCES

1. B. Mikhalkin, H. J. Payne, and L. Isaksen. Estimation of Speed from Presence Detectors. In *Highway Research Record 388*, HRB, National Research Council, Washington, D.C., 1972, pp. 73–83.
2. N. E. Nahi and A. N. Trivedi. *Simultaneous Recursive Estimation of Section Density and Average Speed Using Presence Detector Data*. USCEE Report 420, University of Southern California, Los Angeles, April 1972.
3. H. J. Payne, W. A. Thompson, and L. Isaksen. Design of a Traffic-Responsive Control System for a Los Angeles Freeway. *IEEE Transactions on Systems, Man, and Cybernetics*, Vol. SMC-3, No. 3, May 1973.
4. H. J. Payne. *Analysis and Evaluation of Estimators of Traffic Parameters, Final Report, Part II*. USCEE Report 463, University of Southern California, Dec. 1973.
5. D. C. Gazis, and M. W. Szeto. Design of Density-Measuring Systems for Roadways. In *Transportation Research Record 495*, TRB, National Research Council, Washington, D.C., 1974, pp. 44–52.
6. H. J. Payne, D. Brown, and J. Todd. *Demand Responsive Strategies for Interconnected Freeway Ramp Control Systems, Volume I: Metering Strategies*. Report R-033-84. VERAC Incorporated, San Diego, Calif., March 1985.
7. H. J. Payne and C. Wolfe. Macroscopic Simulation for Urban Traffic Management, The TRAFLO Model, General Technical Specifications, Supplement: Macroscopic Freeway Model. Report ES-R-B001-2, ESSCOR, San Diego, Calif., Oct. 1978.
8. D. A. Wicks and E. B. Lieberman. *Development and Testing of INTRAS, a Microscopic Freeway Simulation Model, Volume I: Program Design, Parameter Calibration, and Freeway Dynamics Component Development*. Report FHWA-RD-76-76. FHWA, U.S. Department of Transportation, May 1977.
9. A. H. Jazwinski. *Stochastic Processes and Filtering Theory*. Academic Press, Inc., Orlando, Fla., 1970.

Publication of this paper sponsored by Committee on Traffic Flow Theory and Characteristics.